Applied Meteorology Unit (AMU)
Quarterly Update Report
First Quarter FY-95

Contract NAS10-11844

31 January 1995

ENSCO, Inc.
445 Pineda Court
Melbourne, Florida 32940
(407) 853-8201 (AMU)
(407) 254-4122

Distribution:

NASA HQ/ME/J. Ernst (2)
NASA HQ/Q/F. Gregory
NASA JSC/MA/B. Shaw
NASA KSC/TM/R. Sieck
NASA KSC/MK/L. Shriver
NASA KSC/CD/R. Crippen
NASA KSC/TM-LLP/R. Tharpe
NASA KSC/TM-LLP-3 /J. Madura
NASA KSC/TM-LLP-3/F. Merceret
NASA KSC/DE-TPO/K. Riley
NASA KSC/EX-NAM-A/P. McCalman
NASA KSC/TE-ISD/C. Lennon
NASA JSC/ZS8-SMG/F. Brody
NASA JSC/DA8/M. Henderson
NASA MSFC/SAO1/R. Eady
NASA MSFC/EL02/K. Hill
Phillips Laboratory, Geophysics Division/LY/R. McClatchey
Hq Air Force Space Command/DOGW/A. Ronn
Hq AFMC/J. Hayes
Hq AWS/CC/F. Misciasci
Hq USAF/XOW/T. Lennon
45th Weather Squadron/CC/T. Adang
45 RANS/CC/R. Reynolds
45 OG/CC/G. Waltman
45 LG/CC/F. Gervais
45 LG/CCR/R. Fore
SMC/SDEW/S. Simcox
Hq AFSPACECOM/DOGW/J. Schattel
AFSPC/DRSR/M. Treu
CSR 1330/M. Maier
SMC/CW/OLAK/D. Carroll
SMC/CW/OLAK/L. Formanek
SMC/CW/OLAK/C. Fain
SMC/CW/OLAK/D. Sandburg
SMC/CW/OLAK/R. Bailey
SMC/CW/OLAK (PRC) /P. Conant
Office of the Federal Coordinator for Meteorological Services and Supporting Research
NOAA W/OM/L. Uccellini
NOAA/OAR/SSMC-I/J. Golden
NOAA/ARL/J. McQueen
NWS Melbourne/B. Hagemeyer
NWS W/SR3/D. Smith
NSSL/D. Forsyth
NSSL/C. Doswell
NWS/W/OSD5/B. Saffle
NWS/W/OSD23/D. Kitzmiller

NWS/EFF/M. Branick
PSU Department of Meteorology/G. Forbes
FSU Department of Meteorology/P. Ray
N.C. State Department of Marine, Earth, & Atmospheric Sciences/S. Koch
N.C. State Department of Marine, Earth, & Atmospheric Sciences/W. Bauman
30th Weather Squadron/CC/R. Miller
30th Weather Squadron/DOS/S. Sambol
45SPW/SESL/D. Berlinrut
SMC/CLGR/L. Palermo
ITT/FSC/T. Wilfong
NOAA/ERL/FSL/J. McGinley
Halliburton/NUS Corp./H. Firstenberg
ENSCO ARS Div. V.P./J. Pitkethly
ENSCO Contracts/S. Leigh

1. Background

The AMU has been in operation since September 1991. Brief descriptions of the current tasks are contained within Attachment 1 to this report. The progress being made in each task is discussed in Section 2.

2. AMU Accomplishments During the Past Quarter

The primary AMU point of contact is reflected on each task and/or subtask.

2.1. Task 001 Operation of the AMU (Dr. Taylor)

Development of Forecaster Applications (Mr. Wheeler)

Mr. Wheeler continued development of the F-Key menu shells for the Shuttle Weather Officer (SWO) Meteorological Interactive Data Display System (MIDDS) terminal. Thus far, menus in support of daily operations and Titan, Delta, Atlas, and Shuttle launch operations have been completed. Mr. Priselac has tested the Shuttle Weather Officer (SWO) menu shells and recommended a few changes that will be incorporated into the final version of the Shuttle menus. The Launch Weather Officer (LWO) for Atlas and Delta support has requested that some additional commands and options be added to the menu shells supporting those operations. Modifications to the launch vehicle menu shells will be completed in January. Menu shells to support Navy operations and the Shuttle ferry flight are under development and should also be completed early in 1995.

Mr. Wheeler also changed the RWO MIDDS terminals to display GOES 8 satellite imagery and developed and installed menus shells and utilities to assist in accessing the Mesoscale Atmospheric Simulation System (MASS) model output now available within the MIDDS. The terminal modifications to accommodate GOES 8 imagery were accompanied by MIDDS utilities that reconfigure the terminals to display GOES 7 images if that should become necessary. The MIDDS terminals cannot switch between displaying GOES 8 and GOES 7 images without adjustments to their settings. Currently, Mr. Wheeler is developing a MIDDS utility that will use bands 2 and 4 of the GOES 8 imagery for nighttime fog display.

The utilities for accessing MASS model output generate 4-panel graphics of surface and 700 mb parameters for analysis and review by the RWO, SMG, and Melbourne National Weather Service Office (NWSO). Since the model is undergoing evaluation, MASS model forecast output is sent to the MIDDS only after the forecast has expired.

Finally, Mr. Wheeler and Ms. Schumann drafted a proposed configuration management plan for the McBasi menu systems installed on the RWO terminals. Major Thorp, Commander, RWO Flight, approved the plan and requested it be implemented. Key points within the plan include the following:

- The AMU will maintain production copies of the McBasi menu systems on AMU hardware.

- One to two days prior to launch, Mr. Wheeler will work with the LWO to ensure any MIDDS system changes have not affected the use of the menus.

- Requests for changes or additions to menu systems will be channeled to Mr. Wheeler through the RWO Flight Commander in order to ensure consensus on the requested changes.

- Finally, Mr. Wheeler will assume sole responsibility for modifying the menu systems.

Mr. Wheeler adhered to the pre-operation steps in the configuration management plan prior to the Titan operation in December. All systems and menu shells were in the correct configurations and worked without incident during the Titan IV launch weather support.

SLF Downrush Wind Event, 16 August 1994 (Mr. Wheeler)

After several strong, convective wind gust events occurred near the Shuttle Landing Facility (SLF) on 16 August 1994, the 45th Weather Squadron requested that the AMU determine whether or not the events were microbursts. Mr. Wheeler completed his analysis of the 16 August 1994 downrush wind events in November 1994 and distributed his results in a memorandum to RWO, SMG, and the Melbourne NWSO. Mr. Wheeler and Mr. Scott Spratt of the NWSO, Melbourne, Florida are now collaborating on reworking the downrush wind event memorandum into a NWS Technical Attachment that will be submitted to the NWS Southern Region for publication.

The following paragraphs summarize Mr. Wheeler's analysis of the meteorological data sets available during the severe weather events.

On 16 August 1994, the KSC and CCAS area experienced several strong downrush wind events. The events started at 2000 UTC near the Indian River side of the NASA causeway and moved east-northeastward across KSC by 2100 UTC. The strongest wind gusts were reported at the Shuttle Landing Facility (SLF) between 2030 and 2050 UTC.

At least two of the local storms that day met the criteria experts (Atkins and Wakimoto 1991 and Fujita 1985) have established as microburst signatures. Those signatures are: 1) the difference between the equivalent potential temperature at the surface and the minimum value aloft is greater than 20˚K, 2) the main precipitation core (defined as radar reflectivities $\geq$ 55 dBz) reaches the level of the minimum equivalent potential temperature, and 3) the divergent outflow pattern and surface area extent is less than 4 km (2.5 miles).

The equivalent potential temperature profile from the late morning Cape rawinsonde sounding is characterized by a large decrease in the equivalent potential temperature in the lowest 4.3 km (14000 ft) of the atmosphere (see Figure 1). This type of environment is conducive for microburst development.

Further, analysis of the WSR-88D vertical radar reflectivity values show that the main precipitation core reached an altitude of 4.3 km (14000 ft), the level of the dry air. These two post analyses indicate that the local storms met Atkins' and Wakimoto's criteria for

their classification of wet microburst events found during the MIcroburst and Severe Thunderstorm (MIST) project in northern Alabama.

The wind tower plots during the time of the microbursts (2030 and 2048 UTC) indicate a starburst divergent pattern with a diameter less than 4 km (2.5 miles). Time versus individual tower wind speed profiles were also similar to what Fujita found typical of microburst events (i.e. a mound-shaped appearance lasting 2 to 5 minutes) (see Figure 2).

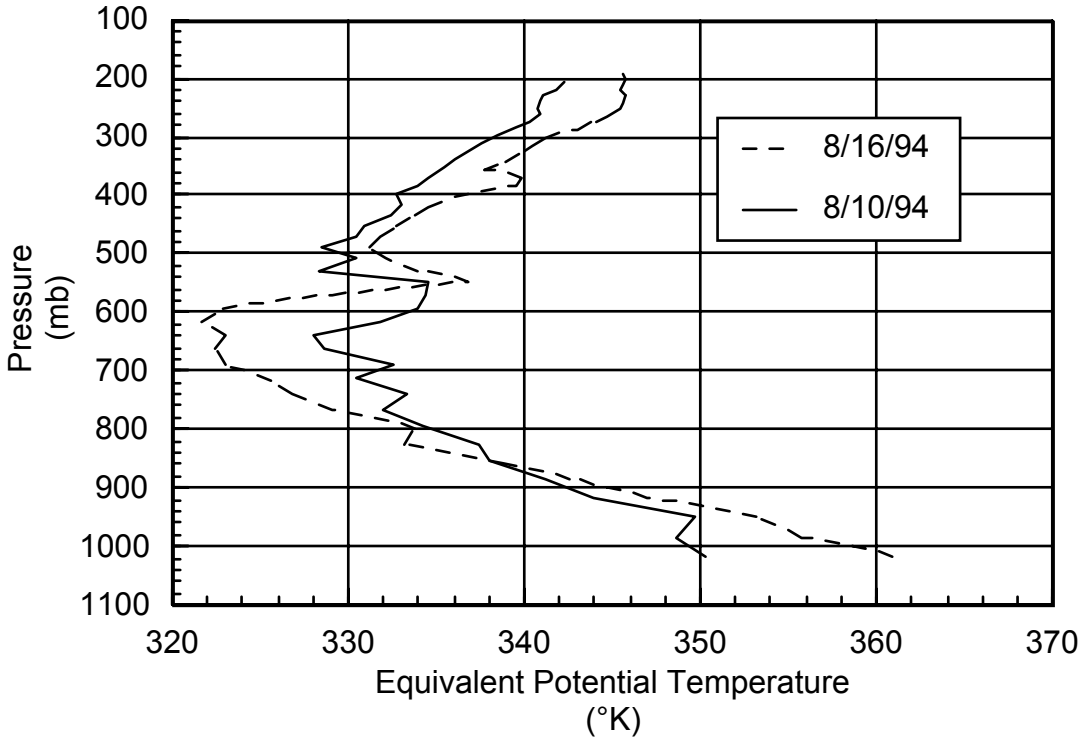

Figure 1. Equivalent potential temperature versus height for 10 and 16 August 1994.

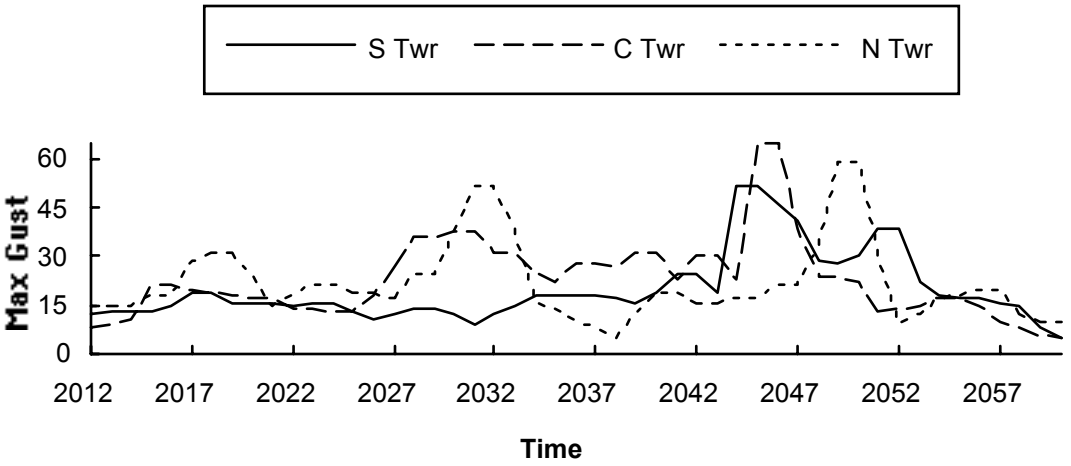

Figure 2. SLF wind speed profiles between 2012 and 2100 UTC on 16 August 1994

Analysis of the 1 minute wind data during the downrush event from each wind sensor, listed in Table 1, indicates the following:

- The north SLF wind sensor reported a shift to a more south-southwest flow (156˚ - 195˚) with a gust of 30.4 ms^{-1} (59 kts),
- The center SLF wind sensor reported a wind shift of only 14˚ (184˚ - 198˚) and a gust of 33.5 ms^{-1} (65 kts), and
- The south SLF wind sensor reported a more northwesterly shift in wind direction (246˚ - 279˚) and a gust of 26.8 ms^{-1} (52 kts) indicating a starburst (divergent) wind pattern.

Table 1. SLF Wind Tower Measurements

ID	Time (UTC)	Direction (˚)	Speed (ms^{-1})	Gust (ms^{-1})
North, 513	2047	153	6.2	10.8
	2048	156	8.2	17.5
	2049	156	13.4	30.4
	2050	195	13.4	30.4
Center, 512	2043	208	9.8	15.4
	2044	184	6.7	11.0
	2045	198	15.0	33.4
	2046	208	15.0	33.4
South, 511	2042	254	7.2	12.9
	2043	246	5.1	9.8
	2044	258	10.8	26.8
	2045	279	16.0	26.8

In Figure 1, the profile of equivalent potential temperature has been plotted for the 16 August 1994 event and compared to that of a normal thunderstorm day (10 August 1994). The difference between the equivalent potential temperature at the surface and that aloft in the 16 August profile exceeds the microburst day criteria of 38˚C, whereas the equivalent potential temperature profile for 10 August shows a difference between the equivalent potential temperature at the surface and the minimum equivalent potential temperature aloft of only 14˚C. The above result coupled with the findings of Atkins and Wakimoto indicate that a forecaster could use this method to differentiate between active and non-active wet microburst days.

During the summer weather regime, a morning and afternoon sounding are necessary to determine changes in the atmosphere that could affect forecasts of thunderstorm activity increases or decreases and their potential severity. Using profiles of equivalent potential temperature, a forecaster should be able to differentiate between an environment capable of supporting thunderstorms associated with wet-microbursts and an environment capable of supporting only typical summer Florida thunderstorms.

Based on the previous investigation, a MIDDS utility should be developed that provides the forecaster a profile of equivalent potential temperature.

References

Atkins, N. T. and R. M. Wakimoto, 1991: Wet microburst activity over the Southeastern United States: Implications for forecasting., *Wea. Forecasting*, **6**, 470-482.

Fujita, T. T., 1985: The downburst. SMRP Res. Paper No. 210, NITIS PB 85-148880. 122 pp. [Available from University of Chicago, Chicago, IL].

2.4. Task 004 Instrumentation and Measurement (Dr. Taylor)

Subtask 3 50 MHz Doppler Radar Wind Profiler (Ms. Schumann)

The Eastern Range contractor, CSR, has installed and tested the MIDDS decoder for the reformatted data from the 50 MHz Doppler Radar Wind Profiler (DRWP). New wind profiles from the 50 MHz DRWP are now available within the MIDDS every 5 minutes.

Captain Scot Heckman of the 45th Weather Squadron provided operational DRWP support during the launch attempt and subsequent launch of a Titan 4 on 20 and 22 December. Ms. Schumann was available for assistance on an on-call basis within RWO during the entire countdown.

Subtask 4 Lightning Detection and Ranging (Ms. Schumann)

The Lightning Detection And Ranging (LDAR) task plan has been distributed to SMG, RWO, Melbourne NWSO, TE-ISD (the LDAR development team), and Dr. Greg Forbes of Pennsylvania State University. The AMU has received concurrence from all parties on the plan for developing a computer based training course, a hard copy users manual, and an instructional video on the use and interpretation of LDAR.

Subtask 5 WSR-88D Evaluation (Mr. Wheeler)

Mr. Wheeler attended the first WSR-88D (NEXRAD) Users' Conference at Norman, Oklahoma from 11-14 October. During the conference, users and Operational Support Facility (OSF) personnel presented very useful NEXRAD radar information and interpretation techniques. There were over 250 attendees and sessions covered a myriad of subjects from severe weather, NEXRAD system operations, user applications to future improvements in the WSR-88D.

Mr. Wheeler began drafting a memorandum describing the potential direction of the WSR-88D tasking. This memorandum will be distributed by mid January.

Subtask 9 Boundary Layer Profilers(Dr. Taylor)

The Air Force is currently procuring a network of boundary layer profilers for the Cape Canaveral Air Station (CCAS)/Kennedy Space Center (KSC) area to support

- Thunderstorm forecasting,
- Mesoscale model initialization,

- Range Safety models (toxic and overpressure dispersion), and
- Wind and temperature monitoring.

The network is being designed and developed by NYMA, Inc. and is based on the LAP - 3000 Doppler radar wind profiler developed by Radian Corporation and Sonoma Technology under a Cooperative Research and Development Agreement (CRDA) with NOAA. The LAP - 3000 radar has an operating frequency of 915 MHz, a peak power of 500 watts, and a five beam electrically steered phased-array antenna with clutter fence. The profilers will provide wind estimates from approximately 120 m to 2 to 4 km above the surface with range gate spacing of 60 to 400 m and averaging periods of 3 to 60 minutes. Radian claims the wind speed accuracy to be ~1 ms^{-1} and the wind direction accuracy to be ~10.

In addition to wind profiles, each radar will contain a Radio Acoustic Sounding System (RASS) which uses four acoustic horns to provide profiles of virtual temperature from approximately 120 m to 1.5 km above the surface. Radian claims the virtual temperature accuracy to be ~1 C.

Although the system is being designed to support up to 15 profilers, the initial configuration of the network will contain five profilers installed in a diamond-shaped pattern centered on KSC (Figure 3.). The first profiler was installed at the False Cape site in October 1994 and the second profiler was installed at the South Cape site in January 1995. Profilers are to be installed at the remaining three sites by the summer of 1995. NYMA is currently designing and developing a system to ingest, process, and display data from all five profilers.

Results from a preliminary analysis of wind estimates from the False Cape profiler are presented in the following paragraphs. The analysis is based on a comparison of 10 minute consensus averaged wind profiles from the 915 MHz profiler and 11 time-proximate rawinsonde profiles from CCAS weather station during the period 01-04 December 1994 (the CCAS weather station is approximately 14 km south-southeast of the False Cape profiler). During this period, the profiler was operated in a three beam configuration producing a 10 minute consensus averaged profile using 8 samples with a first gate height of 276 m and a gate spacing of 193 m. For the analysis the profiler wind estimates were interpolated to the rawinsonde data levels.

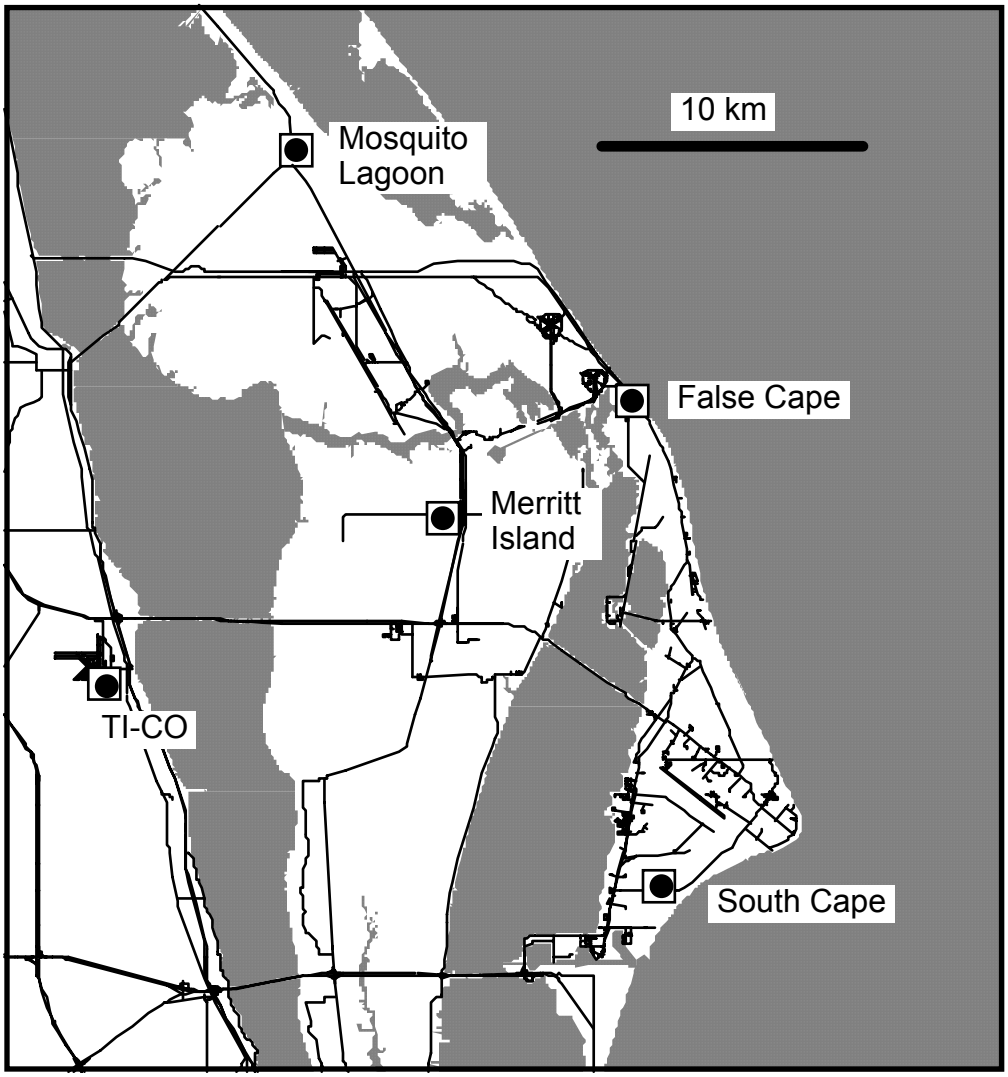

Figure 3. Map illustrating the locations and names of the five Doppler radar wind profilers being installed at KSC/CCAS.

Histograms of the u-component, v-component, and vector differences between the profiler and rawinsonde data are illustrated in Figures 4, 5, and 6. The majority of the component and vector differences are less than 2 ms^{-1}. Component and vector differences of up to 2 ms^{-1} are expected based on the stated accuracy of the profiler and the spatial and temporal sampling differences between the two systems. The component and vector differences of concern are those greater than 2 ms^{-1} and, in particular, those differences of 4 ms^{-1} or greater. In order to understand the reasons for these differences, we examined all 11 time proximate u- and v-component profile pairs. Although some of the large component and vector differences between the profiler and rawinsonde data may be due to wave motions in the atmosphere, part of the large differences are a result of erroneous wind estimates from the profiler.

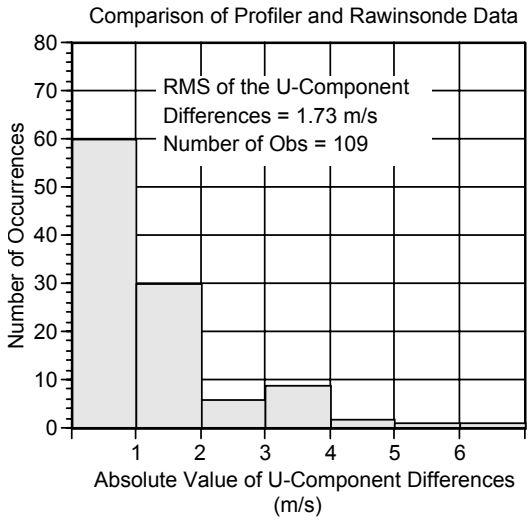

Figure 4. Histogram of the absolute value of the u-component differences between the False Cape wind profiles and the time-proximate CCAS rawinsonde profiles.

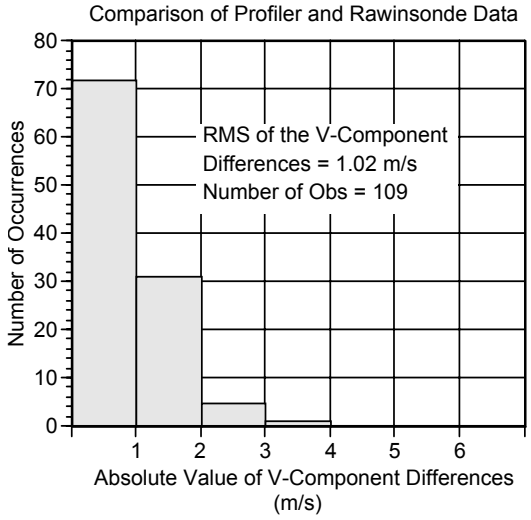

Figure 5. Histogram of the absolute value of the v-component differences between the False Cape wind profiles and the time-proximate CCAS rawinsonde profiles.

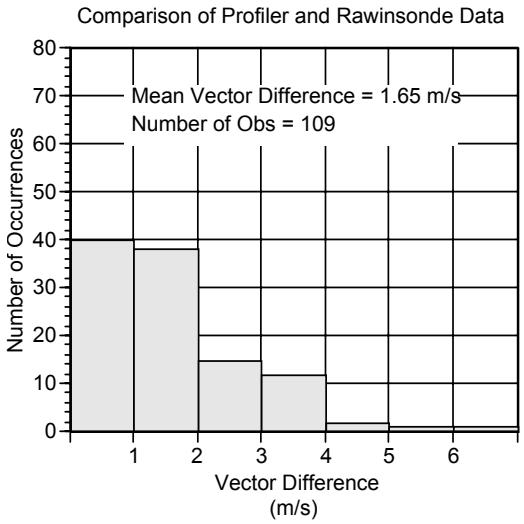

Figure 6. Histogram of the vector differences between the False Cape wind profiles and the time-proximate CCAS rawinsonde profiles.

Two different types of erroneous profiler data are illustrated in Figures 7 and 8. The first type of erroneous profiler data (Figure 7) is a result of a weak atmospheric signal at higher altitudes. In this case, the system was able to produce a consensus averaged wind at a few levels above 3200 m, yet the resulting consensus averaged signal-to-noise (SNR) is less than -12 dB (i.e., a weak atmospheric signal) for the east and vertical beams. It is evident from Figure 7 that the system has selected incorrect signal peaks (i.e., an interference signal as opposed to the atmospheric signal) in the vertical and/or east beam data resulting in erroneous u-component wind estimates in at least one, if not three, of the altitudes above 3200 m.

The second type of erroneous profiler data is illustrated in Figure 8. In this case, the v-component profiler wind estimate at the 469 m altitude is erroneous. This is a result of the system incorrectly selecting a strong persistent side lobe return instead of the atmospheric signal in the north beam data. Examination of 6 other consensus averaged wind profiles within $\pm$ 45 minutes of the 1105 UTC profile indicate that the erroneous wind estimate was present at the 469 m altitude in one of the six profiles.

Although the data set analyzed is too small for producing conclusions about profiler performance, the analysis does suggest that the profiler is performing as expected and indicates a need for post-processing quality control of the wind estimates and/or more advanced signal processing techniques.

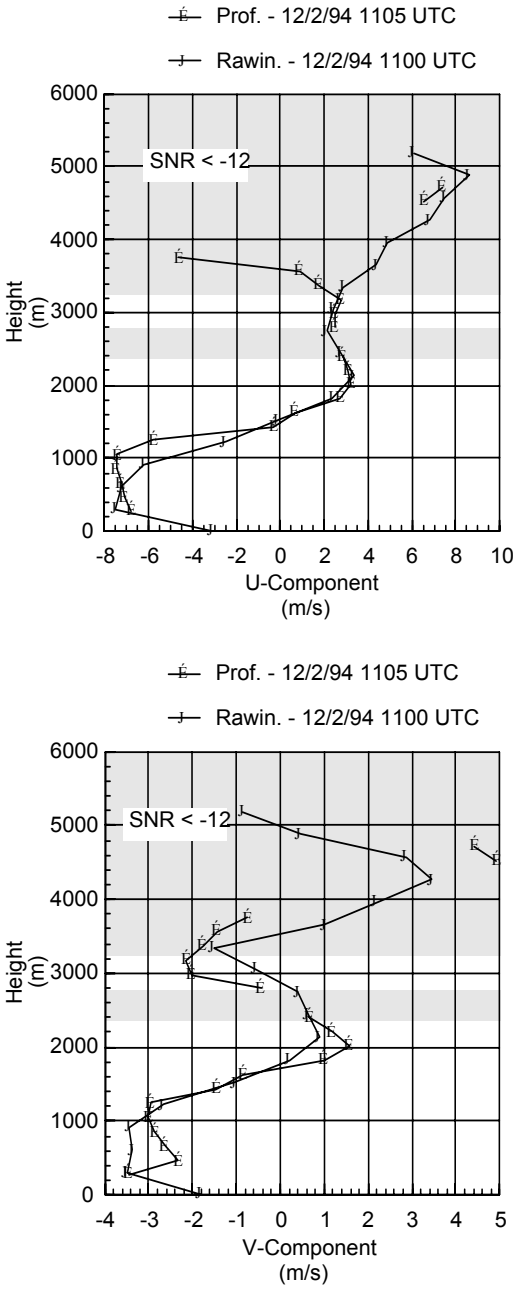

Figure 7. Time proximate u-component and v-component profiles from the False Cape profiler and the CCAS rawinsonde from 02 December 1994. The shaded regions represent altitudes where the consensus average signal-to-noise (SNR) of at least one of the three beams is less than -12 dB.

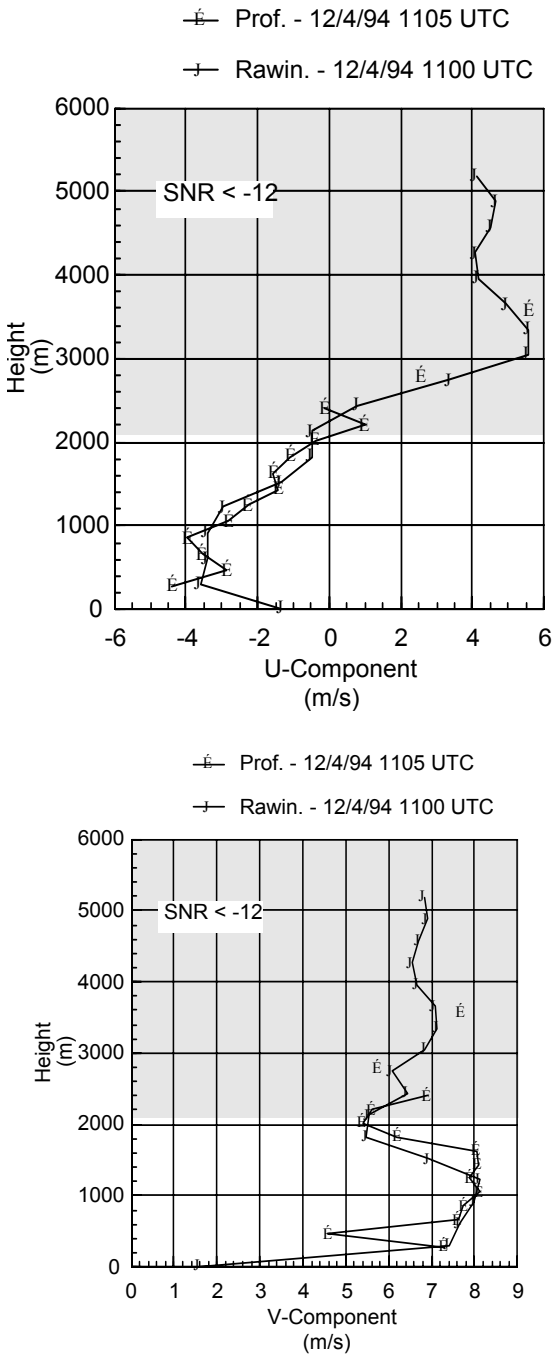

Figure 8. Time proximate u-component and v-component profiles from the False Cape profiler and the CCAS rawinsonde from 04 December 1994. The shaded regions represent altitudes where the consensus average SNR of at least one of the three beams is less than -12 dB.

Subtask 2 Install and Evaluate MESO, Inc.'s MASS Model (Dr. Manobianco)

The archiving of real-time MASS model runs for the purpose of model evaluation is complete. All available coarse and fine grid forecasts and observations from 15 January 1994 through 15 October 1994 are being used for model verification. The AMU continues to run MASS in real-time so that model initialization and forecast products can be transferred back to MIDDS for examination by RWO, SMG, and NWS forecasters. In addition, the model runs are still being archived so that Model Output Statistics (MOS) can be generated from the largest possible sample of real-time cases.

The transfer of MASS output to MIDDS occurs after the forecasts have expired so that initialization and forecast products can not be used for operational decisions. In November 1994, Dr. Manobianco distributed a memorandum to RWO, SMG and NWS detailing the availability of MASS initialization and forecast output in MIDDS. Dr. Manobianco also contacted Major Robert Thorp at RWO, Ms. Doris Rotzoll (Techniques Development Unit) at SMG, and Mr. David Sharp (Science Operations Officer) at NWS to discuss the MASS data transfer and the specific feedback that the AMU would like to receive regarding the content, utility, and format of numerical products from MASS. For example, Mr. Bud Parks (RWO) is now using MASS model output as guidance in preparing simulated Terminal Area Forecasts for TTS from daily 0000 UTC 45 km runs that are available 5 minutes after the MASS forecast products have expired.

MASS Real Time Run Statistics

Ms. Yersavich has processed data to yield statistics on the number of completed MASS model runs compared with the number of total possible runs for the entire archiving period from January through October 1994. This analysis provides the percentage of failed runs and categorizes these runs based on problems with the systems (hardware/software) or data. Figure 9 displays these results as pie charts. There were a total of 462 complete 45 km (coarse grid) runs and 440 complete 11 km (fine grid) runs out of a total 548 possible runs. When the coarse and fine grid runs both failed, the coarse grid forecasts were sometimes executed in place of the fine grid forecasts. As a result, the number of complete 45 km and 11 km forecasts do not match exactly.

Figure 9 illustrates that 10.9% of the coarse runs were lost due to hardware problems, 2.4% due to software problems, and 2.4% due to loss of data. The hardware problems were related to disk and power supply failures while the software problems were related to changing the procedures that handle data processing. The loss of data includes only Nested Grid Model (NGM) gridded data that are required as first guess fields in the MASS pre-processor. Figure 9 also shows that of the 462 complete 45 km runs, 425 (92%) used NGM analysis grids valid at the time model initialization, while 37 (8%) used NGM forecast grids from the previous (12-h old) forecast cycle.

The 13.1% (2.4% + 10.9%) of the 45 km runs lost due to hardware and software problems could have been prevented by using a backup system and not changing the real-time UNIX scripts that process data. In that case, 97.6% of the 45 km runs could have been completed. Furthermore, if alternate data sets such as Eta or Medium Range

Forecast (MRF) gridded data were used, all possible 45 km forecasts could have been completed. No model forecasts were lost due to instabilities generated by the model's physics or dynamics since December 1993 when the AMU started running MASS in a real-time configuration. These results suggest that MASS is extremely robust and would be a very reliable operational system.

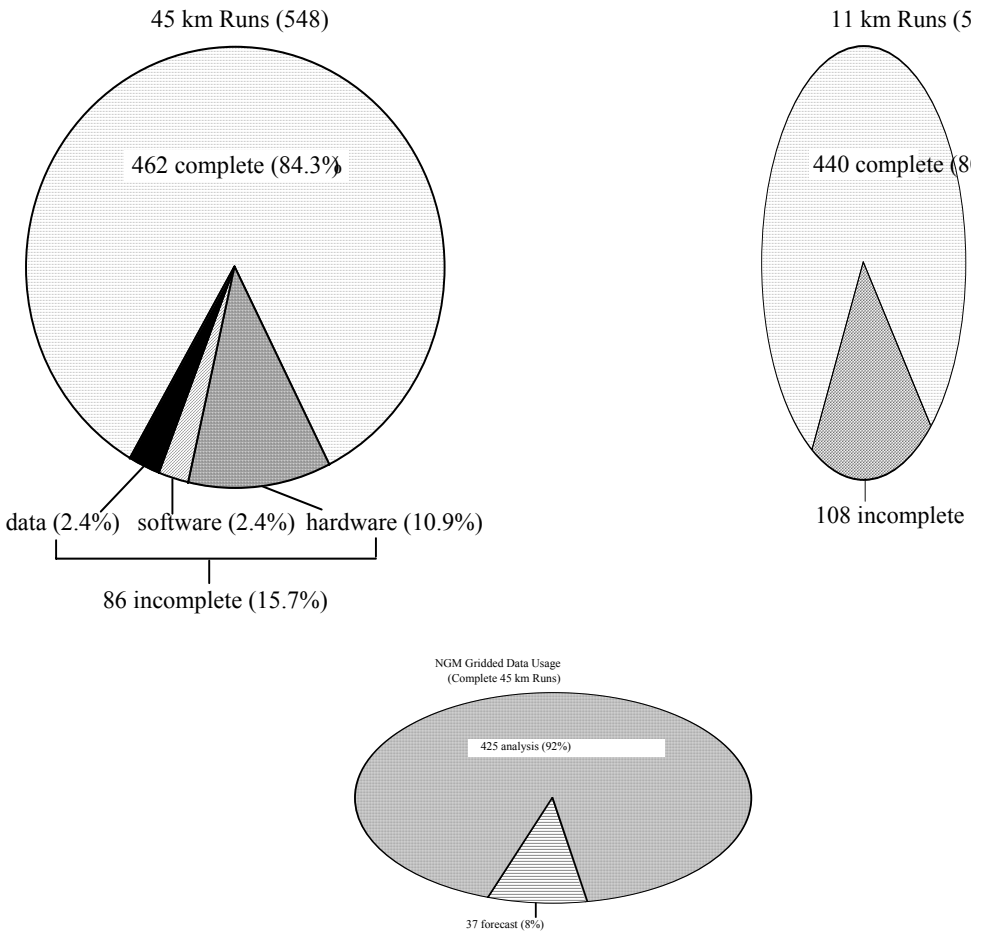

Figure 9. Pie charts showing the percentage of complete 45 km runs, complete 11 km runs, and NGM gridded data usage for complete 45 km runs.

MASS Evaluation at Rawinsonde Sites

Dr. Manobianco completed the analysis of MASS model forecast errors at three rawinsondes sites in Florida for 45 km and 11 km MASS runs, NGM B-grid (~190 km) runs, and persistence forecasts for the entire archive period. He also examined MASS model forecasts of stability indices and precipitable water for the same period. Dr. Manobianco presented these results at the Sixth Conference on Aviation Weather Systems held in Dallas, TX from 15-20 January 1995. The subsequent sections summarize material from the paper he presented in Dallas co-authored with Dr. Taylor and Dr. John Zack (MESO, Inc.) entitled "Forecast Skill of A High Resolution Real-Time Mesoscale Model Designed for Weather Support to Operations at the Kennedy Space Center and Cape Canaveral Air Station".

Methodology

The analyses and forecast fields from all available coarse grid, fine grid, NGM, and persistence forecasts from 15 January 1994 through 15 October 1994 are bilinearly interpolated to the rawinsonde station locations at West Palm Beach, FL, Tampa Bay, FL,

and Cape Canaveral, FL. These sites are selected because they are the only rawinsonde locations contained within the MASS fine grid and coarse grid domains. The NGM and persistence errors are included to provide a benchmark for MASS forecast errors. Note that persistence errors are calculated only at 12 h and 24-h forecast times. Also, fine grid forecasts extend to 12-h so fine grid errors are computed only at 0 h and 12 h.

The two statistical measures used here to quantify model forecast skill are the bias and root mean square error (RMSE) computed from the twice-daily (0000 UTC and 1200 UTC) rawinsonde observations of temperature (˚C), relative humidity (%), and wind speed (ms^{-1}) at 850 mb, 500 mb, and 300 mb. Errors which are greater than two standard deviations from the mean forecast minus observed differences are removed. The errors at each pressure level and forecast time (i.e., 0 h, 12 h, and 24 h) are averaged for all three stations at both 0000 UTC and 1200 UTC verifying times over the entire 10 month period. Therefore, the maximum number of data points (N) used to derive the average bias and RMSE at a given pressure level and time is 1644 (i.e., 548 total possible runs x 3 stations). The actual value of N varies depending on the variable and pressure level and is usually greater than 1000.

Temperature Bias and RMSE

The bias and RMSE in temperature (T) are shown in Figure 10. The coarse and fine grid T bias at 300 mb, 500 mb, and 850 mb are less than 0.25˚C in the initial analyses (Fig. 10a). In contrast, the NGM analyses show a negative (cool) bias at all three levels of more than -0.5˚C. By 12 h, the coarse and fine grid runs develop a cool bias at 500 mb and 300 mb on the order of -1˚C that is slightly larger than the NGM cool bias at this time (Fig. 10c). At 850 mb, MASS runs show a small positive (warm) T bias of less than or equal to 0.5˚C in contrast to the cool bias of -0.75˚C in the NGM runs. The 24-h MASS coarse grid T bias at 500 mb and 300 mb remains negative on the order of -1.0˚C and positive at 850 mb. The persistence forecasts of T at 12 h and 24 h are basically unbiased at all three levels (Figs. 10c, e).

The RMSE in T from coarse and fine grid analyses (0 h) are less than 0.5˚C at 850 mb, 500 mb, and 300 mb. In the 0-h NGM analyses, the RMSE in T are approximately twice as large at all levels compared with those from MASS. At 12 h and 24 h, the RMSE in T from the coarse grid, fine grid, NGM, and persistence forecasts are on the order of 1.0-1.3˚C at all levels. The RMSE in T from MASS forecasts increase most notably between 0 h and 12 h (Figs. 10b, d).

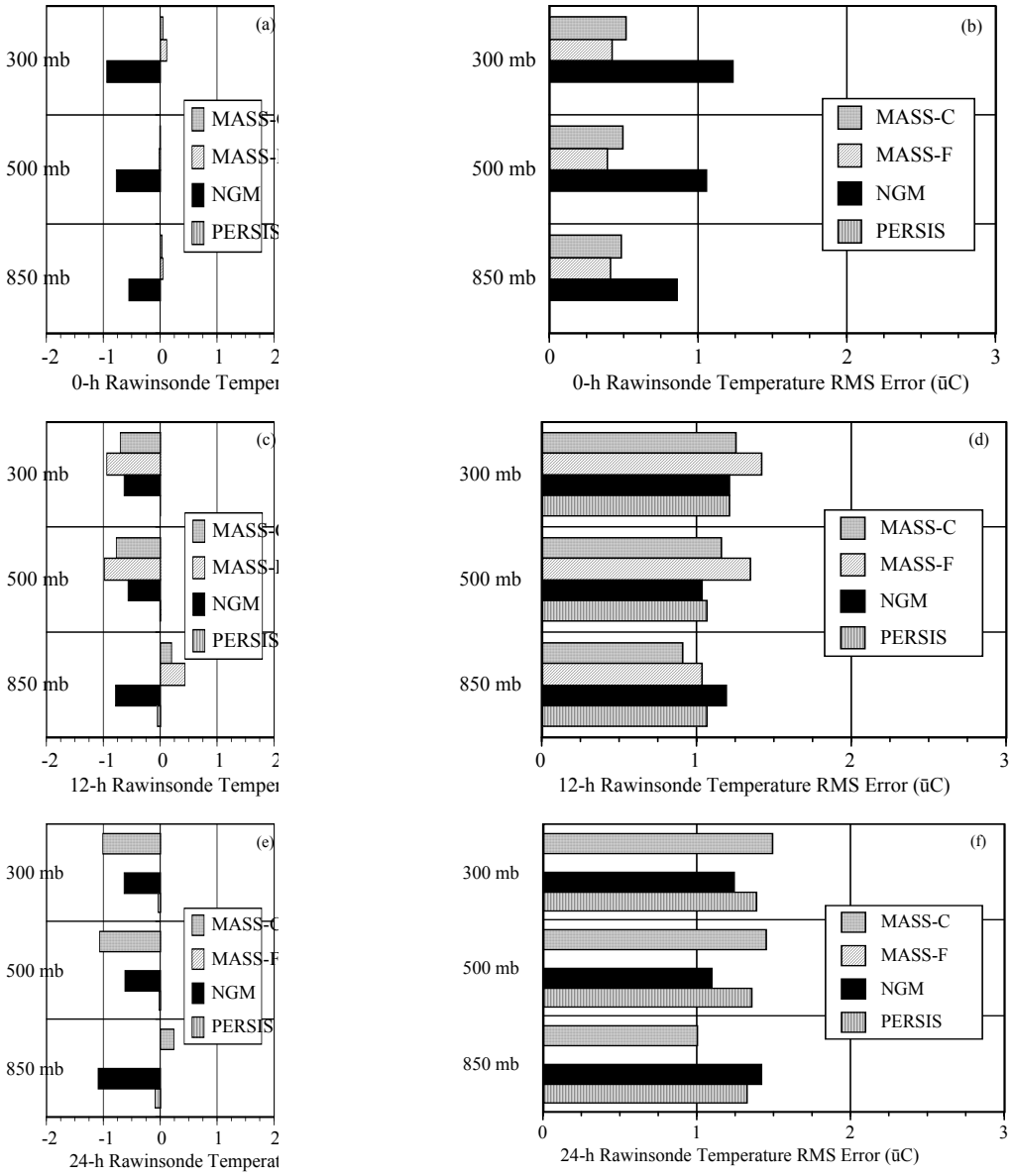

Figure 10. Temperature bias (˚C) plotted at 850 mb, 500 mb, and 300 mb for MASS coarse grid, MASS fine grid, NGM, and persistence forecasts at 0 h in panel (a), 12 h in panel (c), and 24 h in panel (e). Panels (b), (d), and (f) show the root mean square error (RMSE) in temperature at 0 h, 12 h, and 24 h, respectively. Note that persistence errors are computed only at 12 h and 24 h while fine grid forecast errors are computed only at 0 h and 12 h.

Relative Humidity Bias and RMSE

The relative humidity (RH) bias and RMSE in RH are shown in Figure 11. At 300 mb, MASS coarse and fine grid analyses display a negative (dry) bias of about -8% whereas the NGM analyses show a positive (wet) bias on the order of 6% (Fig. 11a). The

wet bias at 300 mb persists in the NGM forecasts increasing to more than 20% by 24 h. In contrast, the coarse grid runs do not maintain the initial dry bias (Figs. 11c, e). However, the fine grid runs develop a wet bias of less than 10% at 300 mb in the 12-h forecasts. An initial small dry (negative) bias at 850 mb in MASS coarse analyses increases to nearly -10% by 24 h. As with T, the persistence forecasts of RH at 12 h and 24 h are basically unbiased at all three levels (Figs. 11c, e).

The RMSE in RH from the MASS and NGM analyses (0 h) range from about 8% to 18% at all three pressure levels and show a tendency to increase with decreasing pressure except for fine grid RMSE in RH at 500 mb (Fig. 11b). The NGM RMSE in RH exceed 30% and are largest in the 24-h forecasts (Fig. 11f). The MASS RMSE in RH are of the same magnitude as those from the NGM at 12 h and 24 h at 850 mb and 500 mb.

Wind Speed Bias and RMSE

Figure 12 displays the wind speed bias and RMSE in wind speed. The NGM and MASS analyses exhibit a negative (slow) bias at all three levels that is maintained at 12 h and 24 h (compare Figs. 12a, c, e). The largest bias occurs at 500 mb in 12-h and 24-h coarse grid and NGM forecasts with values as large as -2 ms^{-1} (NGM 24-h runs, Fig. 12e). The persistence forecasts of wind speed at 12 h and 24 h show a much smaller negative bias compared with the MASS or NGM forecasts at all three pressure levels (Figs. 12c, e).

The evolution of RMSE in wind speed is similar to that for T and RH in that the largest error growth occurs between 0 h and 12 h for MASS coarse and fine grid runs. However, the MASS RMSE in wind speed are consistently less than those from persistence especially at 300 mb where 24-h persistence RMSE exceed 6 ms^{-1} (Fig. 12f).

K Index Errors

This section focuses on MASS model errors in the stability parameter known as the K Index which is defined as:

$$\text{K Index} = T_{850} - T_{500} + Td_{850} - T_{700} + Td_{700}$$

where T stands for temperature (˚C), Td stands for dew point temperature (˚C), and the subscripted numbers refer to pressure levels. Forecasters routinely use the K Index and other stability indices such as the lifted index to assess the potential for convection to occur based on observed and/or forecast values of the quantities that define the indices. The errors in the model's basic prognostic variables such as temperature and moisture are reflected in parameters such as the K Index. However, it may be difficult to understand readily how errors in the components of a particular index affect errors in the index itself. For this reason, the stability index errors are computed directly.

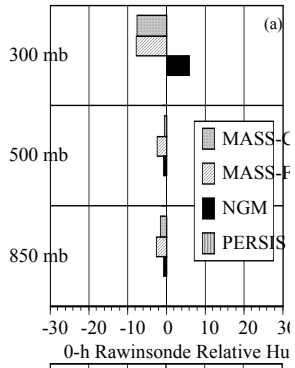
(a)
300 mb
500 mb
850 mb
MASS-C
MASS-F
NGM
PERSIS
-30 -20 -10 0 10 20 30
0-h Rawinsonde Relative Hu

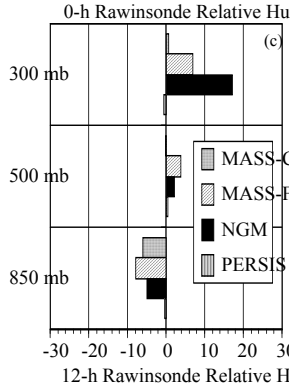
(c)
300 mb
500 mb
850 mb
MASS-C
MASS-F
NGM
PERSIS
-30 -20 -10 0 10 20 30
12-h Rawinsonde Relative H

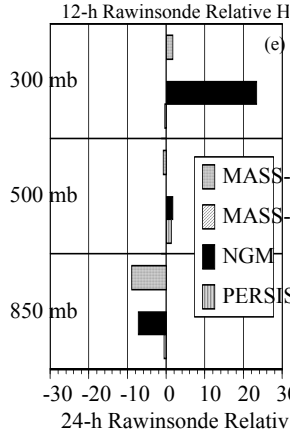
(e)
300 mb
500 mb
850 mb
MASS-
MASS-
NGM
PERSIS
-30 -20 -10 0 10 20 30
24-h Rawinsonde Relativ

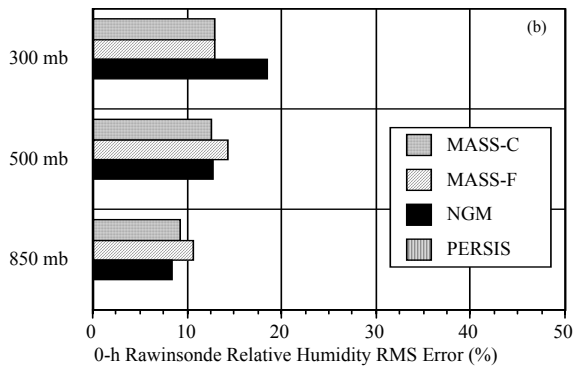
(b)
300 mb
500 mb
850 mb
MASS-C
MASS-F
NGM
PERSIS
0 10 20 30 40 50
0-h Rawinsonde Relative Humidity RMS Error (%)

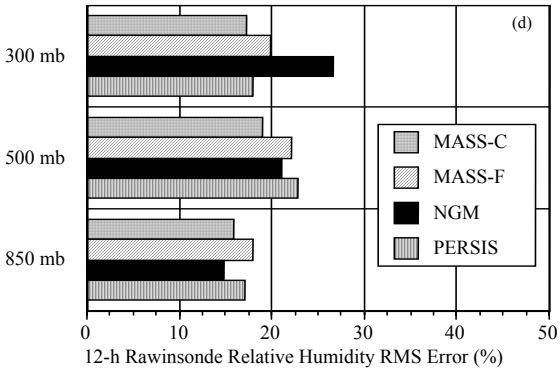
(d)
300 mb
500 mb
850 mb
MASS-C
MASS-F
NGM
PERSIS
0 10 20 30 40 50
12-h Rawinsonde Relative Humidity RMS Error (%)

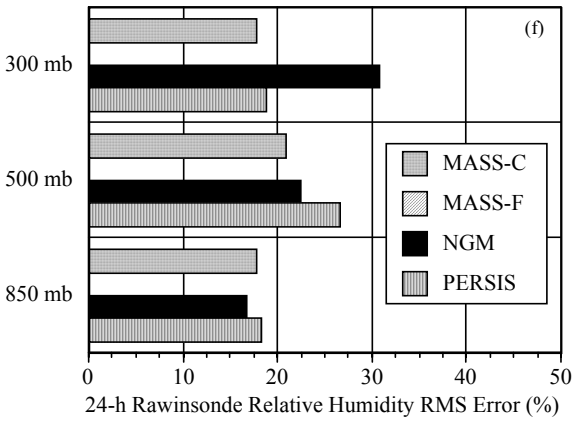
(f)
300 mb
500 mb
850 mb
MASS-C
MASS-F
NGM
PERSIS
0 10 20 30 40 50
24-h Rawinsonde Relative Humidity RMS Error (%)

Figure 11. Relative humidity bias (%) plotted at 850 mb, 500 mb, and 300 mb for MASS coarse grid, MASS fine grid, NGM, and persistence forecasts at 0 h in panel (a), 12 h in panel (c), and 24 h in panel (e). Panels (b), (d), and (f) show the root mean square error (RMSE) in relative humidity at 0 h, 12 h, and 24 h, respectively. Note that persistence errors are computed only at 12 h and 24 h while fine grid forecast errors are computed only at 0 h and 12 h.

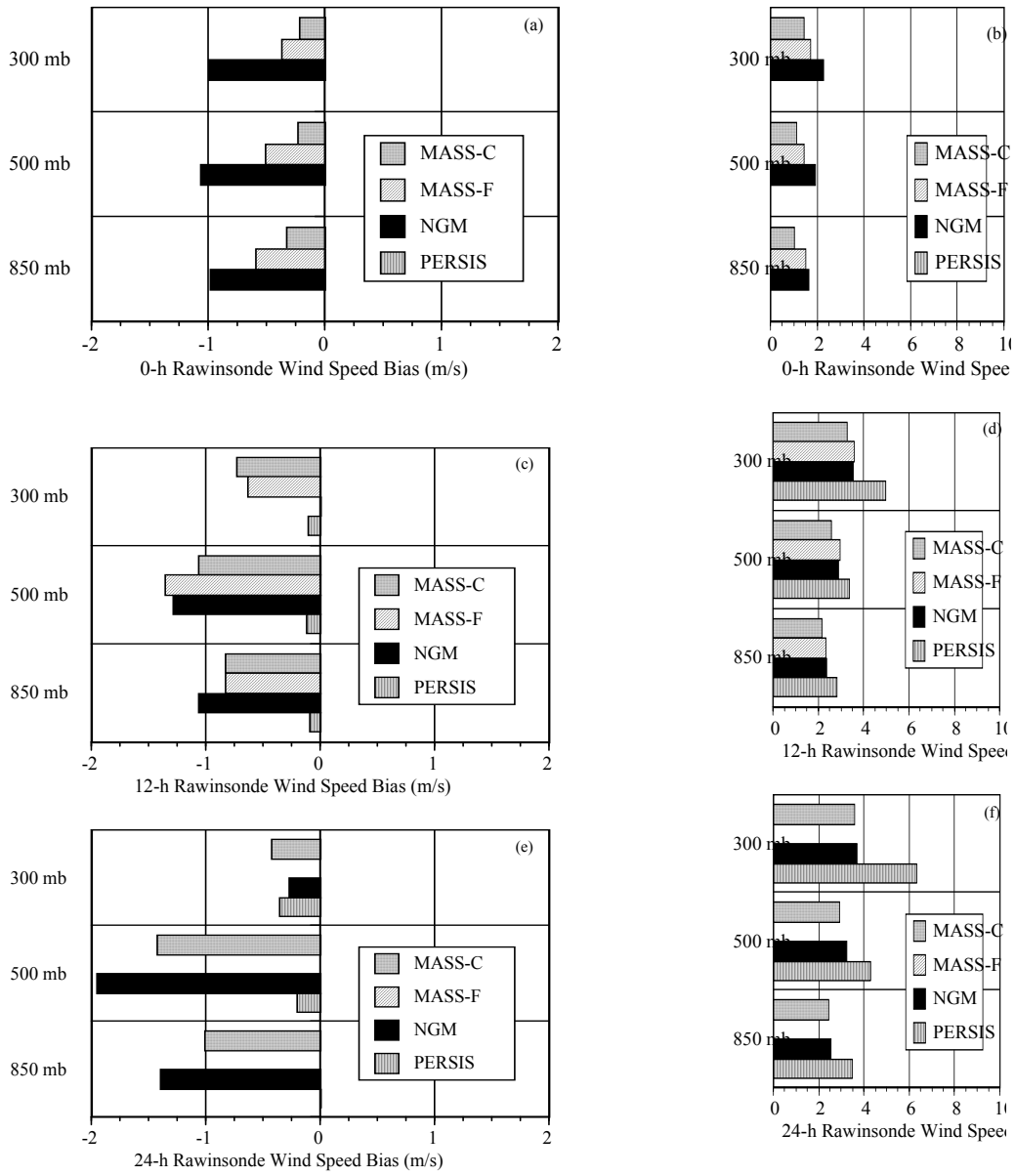

Figure 12. Wind speed bias (ms^{-1}) plotted at 850, 500, and 300 mb for MASS coarse grid, MASS fine grid, NGM, and persistence forecasts at 0 h in panel (a), 12 h in panel (c), and 24 h in panel (e). Panels (b), (d), and (f) show the root mean square error (RMSE) in wind speed at 0 h, 12 h, and 24 h, respectively. Note that persistence errors are computed only at 12 h and 24 h while fine grid forecast errors are computed only at 0 h and 12 h.

Figure 13 displays the observed versus forecast K Index values computed at Tampa Bay, FL from all coarse grid (45 km) runs between 15 January 1994 and 15 October 1994 at the 0-h, 12-h, and 24-h forecast times. The results from the other two stations (i.e. Cape Canaveral, FL and West Palm Beach, FL) and fine grid (11 km) runs are similar and are not shown. At present, the K Index errors from the NGM can not be computed because the on-line archive of NGM gridded data does not contain 700 mb temperature or

moisture information. The larger values of the K Index are indicative of a more unstable atmosphere with values exceeding 40 almost always associated with thunderstorms.

The average bias and RMSE for K Index values less than 20 and greater than or equal to 20 are shown at the lower right hand corner of each graph in Figure 13. The coarse grid runs show a large positive bias reaching 6.8 at 12 h and RMSE of 10.8 by 24 h in K Index for values less than 20. At K Index values of 20 or more, the bias is slightly negative with RMSE that are smaller than those for K Indices less than 20. These results indicate that the model forecasts too much instability (K Index too large) at Tampa Bay, FL when the atmosphere is relatively more stable (i.e., observed values of K Index less than 20). For larger K Index values (i.e. greater instability), the coarse grid K Index forecasts are more accurate and negatively biased meaning that the model underestimates the instability (i.e., K Index too low). A further examination of errors in temperature and moisture errors from the Tampa Bay, FL soundings reveals that more than 95% of the error in 45 km K Index forecasts are due to errors in the dew point temperatures at 850 mb and 700 mb (not shown).

Summary

The average bias and RMSE have been computed from twice daily rawinsonde data for three sites over Florida from 15 January 1994 to 15 October 1994. The MASS model coarse and fine grid analysis (0 h) bias and RMSE for temperature and wind speed are typically smaller than those from the NGM indicating that the MASS analysis scheme fits the rawinsonde data more closely. By 12 h, the errors in the NGM and MASS forecasts for temperature, moisture, and wind at 850 mb, 500 mb, and 300 mb are similar in magnitude. The MASS model predictions of stability based on K Index are more accurate when the soundings are more unstable (i.e. higher K Index values). In general, MASS is predicting the large scale features that are sampled by twice-daily rawinsonde observations as well as the NGM. This result is not surprising since the NGM provides boundary conditions for the coarse grid and the coarse grid provides boundary conditions for fine grid. Under strong inflow conditions, the information introduced at the boundary of the coarse or fine grid domains can impact the forecasts in a relatively short time period.

The higher resolution MASS model should show more skill than current operational models like the NGM in predicting mesoscale features such as the sea breeze. Mesoscale model validation requires mesoscale data. Therefore, the AMU is in the process of verifying the coarse and fine grid forecasts of the sea breeze, convective precipitation, and tropospheric winds above 2 km using hourly measurements from the KSC/CCAS wind towers (~5 km average spacing), Florida Water Management and KSC/CCAS rain gauges (~10 km average spacing), and KSC 50 MHz Doppler wind profiler, respectively.

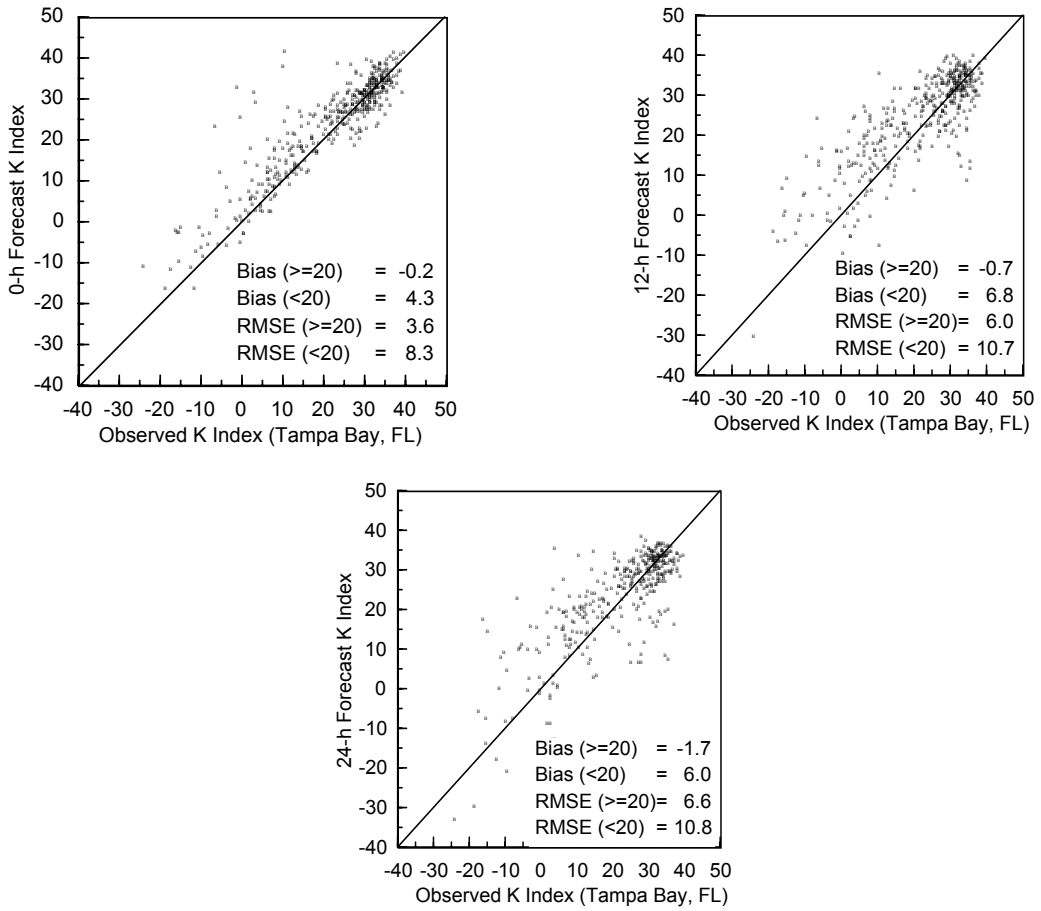

Figure 13. Observed versus forecast K Index values computed at Tampa Bay, FL from all coarse grid (45 km) runs between 15 January 1994 and 15 October 1994 at the 0-h, 12-h, and 24-h forecast times. The line on each graph has a slope of unity indicating perfect forecasts. The bias and RMSE in K Index shown in each graph are computed for values of K Index less than 20 and values of K Index greater than or equal to 20.

Subtask 4 Install and Evaluate ERDAS (Mr. Evans)

The primary AMU activity during the past quarter on the Emergency Response Dose Assessment System (ERDAS) model evaluation was the preparation of a memorandum describing the AMU's modeling of a nitrogen tetroxide release from Complex 41 on 20 August 1994. Excerpts of the modeling analysis are presented here.

At 1426 UTC on 20 August 1994, a nitrogen tetroxide (N_2O_4) pipeline at Titan Complex 41 on Cape Canaveral Air Station (CCAS) ruptured and released 200 to 400 gallons of N_2O_4 vapor into the atmosphere. The AMU used the accident as a case study for evaluating ERDAS' ability to model the release and accurately predict the location and concentration of the plume. We evaluated output from both of the major models within ERDAS–the meteorological model, RAMS (Regional Atmospheric Modeling System), and the diffusion model, HYPACT (Hybrid Particle and Concentration Transport).

Although no measurements were taken of the concentrations within the plume, witnesses observed the brownish-orange plume drift west, rise, and then drift northward offshore during the one to two hour period after the release.

Model Configuration

The RAMS model configuration for ERDAS has been documented in several reports and papers written by Lyons and Tremback. The ERDAS Final Report (Lyons and Tremback, 1994) presents details of the configuration (Section 2.1: Meteorological Modeling). Important features of the model configuration are listed below.

- The horizontal grid spacing of the three nested grids are 60 km (38 ∞ 36 points), 15 km (34 ∞ 38 points), and 3 km (37 ∞ 37 points).
- The vertical grid of 22 points extends to approximately 13.5 km for the 60-km and 15-km grids. The vertical grid of 21 points extends to approximately 3 km.
- The model runs twice daily producing 24 hourly forecasts beginning at 0000 UTC and 1200 UTC.
- The model physics selected for ERDAS do not include clouds, condensation, or precipitation.
- Land use classification of 3-km grid cells were derived from high resolution U. S. Geological Survey digital data bases. Classes include water and 18 land classifications along with percentage of land coverage.

Meteorology on 20 August 1994

On the morning of 20 August 1994, a large high pressure area stretched from the South Carolina area eastward into the Atlantic. The pressure gradient over Florida was very weak as was indicated by the light and variable surface winds which prevailed at most Florida stations. At 1200 UTC, the WINDS system was reporting wind speeds less than 1.5 ms^{-1} at all towers. The analyzed surface wind field from RAMS for 1200 UTC showed light northeasterly flow over CCAS and light north and northwesterly flow over Merritt Island. Data from Tower 313 at 1200 UTC and from the rawinsonde at 0900 UTC showed that the winds above 150 meters were generally from the south at speeds less than 4 ms^{-1}.

During the morning, there was sufficient warming of the surface with the clear skies to produce a sea breeze. Surface winds at Tower 110, located south of Complex 41, were westerly at 1 ms^{-1} at 1300 UTC and then switched to south-southeast at 0.5 ms^{-1} at 1400 UTC. At tower 311, located northwest of Complex 41, the winds went from calm at 1300 UTC to northeasterly at 1 ms^{-1} at 1400 UTC. At tower 509, located southwest of Complex 41, the winds went from southerly at 0.5 ms^{-1} at 1300 UTC to southwesterly at 4 knots at 1425 UTC to south-southeasterly at 1 ms^{-1} at 1505 UTC.

The tower data and the analyzed surface wind field were used to follow the progression of the sea breeze inland during the morning. The analyzed surface wind field was obtained by performing a gridded Barnes analysis on the tower, buoy and surface data. At 1300 UTC the sea breeze had not moved inland as indicated by the westerly wind at Tower 110. Southerly and westerly winds prevailed over most of CCAS and Merritt Island. At 1410 UTC, the winds at Tower 110 switched to southeasterly as the sea breeze moved inland. The analyzed wind field at 1400 UTC (Figure 14) shows weak easterly winds across most of CCAS but not over Merritt Island where winds were from the west. The data from Tower 311 indicates that the sea breeze passed this tower at 1535 UTC as the wind direction shifted from southwesterly to easterly and the temperature dropped from 86°F to 83°F between 1530 and 1535 UTC. The analyzed wind field at 1500 UTC (Figure 15) showed little difference from the 1400 UTC wind field, but by 1600 UTC the winds were easterly over CCAS and most of Merritt Island. By 1600 and 1700 UTC the sea breeze had moved past Merritt Island to the Indian River as weak easterly flow prevailed over all of KSC/CCAS through 1700 UTC.

RAMS Results

We compared the observed data with the modeled data to determine the reliability of RAMS for the day of the N_2O_4 release. The results from the RAMS model were obtained from the run which began at 1200 UTC on 20 August. Figure 16 shows the RAMS-predicted wind field for 10.6 meters (surface) and 254.1 meters for the 1600 UTC. We compared RAMS' three-dimensional meteorological fields with observed data from the various tower levels, surface observation sites, and the 1500 UTC CCAS rawinsonde.

At 1300 UTC, RAMS predicted weak westerly and northwesterly flow over the CCAS area at the surface and aloft as shown in the wind fields at 10.6 and 254.1 meters. There was no significant upward vertical motion over Merritt Island or CCAS except for a small east-west oriented line of convergence located near the southern end of Merritt Island. The direction of the observed wind vectors did not agree very well with the direction of the RAMS-predicted surface wind vectors over most of the grid because the winds were very light over most of the area. However, when winds are light, the directions tend to vary considerably because of the lack of dominant prevailing wind. The wind vectors from the observed and predicted wind fields did agree in the area of northern Merritt Island. Observed winds in the north Merritt Island area were west-northwest at approximately 1 ms^{-1} while the RAMS-predicted winds were northwest at approximately 2 ms^{-1}.

At 1400 UTC, RAMS did not show signs of a sea breeze circulation but decreased the westerly flow over the CCAS land area and Merritt Island as the land surfaces warmed. RAMS predicted light northerly winds at the surface over CCAS while the winds at the grid points on Merritt Island became almost calm. RAMS predicted easterly winds at the height of 254.1 m over CCAS and Merritt Island. The light, near-calm winds predicted by RAMS over CCAS and Merritt Island agreed with the observed winds.

At 1500 UTC, RAMS predicted weak easterly flow over Merritt Island and northern CCAS as it began to generate a sea breeze circulation. Upward vertical motion increased

over CCAS and Merritt Island from 1400 UTC. The observed and predicted wind fields showed good agreement over CCAS and Merritt Island where the winds were very light.

THIS PAGE INTENTIONALLY LEFT BLANK - for Figures 14 and 15

THIS PAGE INTENTIONALLY LEFT BLANK for figure 16

By 1600 UTC, RAMS predicted the winds to increase from the northeast at the 10.6-meter level over northern Merritt Island and CCAS. RAMS did not strengthen the sea breeze circulation which was evident in the 1500 UTC RAMS output. The strength of the updrafts as indicated by the vertical motion fields increased but remained centered over CCAS and Merritt Island (Figure 16). The observed wind field at this time showed that the sea breeze had moved inland to near the Indian River.

At 1700 UTC, RAMS continued the northeasterly winds over the northern CCAS land area and northern Merritt Island. The strength of the updrafts increased from the previous hour but remained located over the center of the CCAS land area and over the center of Merritt Island. The model did not predict any upward motions over the Complex 41 area. RAMS continued to under predict the strength of the surface wind flow compared to the observed wind field. The observed wind field showed an increase in the easterly flow over CCAS.

The 3-km resolution of the land use in the ERDAS configuration significantly affected the RAMS predicted wind fields at Complex 41. The narrow strip of land where Complex 41 is located is approximately 1½ to 4 km wide, bounded on the west by the Banana River and on the east by the Atlantic Ocean. The land use in the area is very complex due to the oceans, estuaries, swamps and vegetated land. RAMS attempts to apply a single land use class and percent land area to each 3 km x 3 km grid square. RAMS classified the grid square where Complex 41 is located as inland water or ocean (Classes 14 and 15) with a percent land fraction of less than 40%. The grid squares surrounding the Complex 41 grid square were classified as bog and marsh (Class 13), evergreen shrub (Class 16), and short grass (Class 2). This inaccurate classification can lead to inaccurate modeling of horizontal and vertical velocities and turbulence.

The narrow strip of land where Complex 41 is located showed no significant upward motion because of the inaccurate land use classification due to the coarse resolution in this area. The coarse resolution resulted in the model's attempting to apply a single land use class (water) and percent land area to the 3 km x 3 km grid area surrounding Complex 41.

HYPACT Results

We ran HYPACT for two different scenarios. The two scenarios were identical except for the release point of each. The basic data input to HYPACT were the following:

Spill Amount:	400 gallons
Chemical:	Nitrogen Tetroxide (N_2O_4)
Pool Size:	500 square feet
Release Rate:	50.0 lbs/min
Release Time:	1426 UTC
Release Duration:	14 minutes
Dispersion Simulation End:	1700 UTC

HYPACT produces predictions of the three-dimensional plume every 10 minutes as it disperses over time. HYPACT models the plume by tracking a large set of particles

released from a designated point or area. HYPACT transports and disperses the particles using the RAMS-predicted wind fields and displays the plume locations by overlaying the particles on maps and vertical cross-sections. HYPACT calculates pollutant concentrations based on the particle dispersion. The concentration calculation function, however, does not currently work in ERDAS and is being corrected by ASTER/MRC.

For this release, the simulated plume behaved like a single puff rather than a continuous plume because of the short 14-minute release time.

Complex 41 Release Point

For the first HYPACT simulation, we modeled the release from its actual release location at Complex 41. The actual land use in the area is very complex due to the oceans, estuaries, swamps and vegetated land in the area. However, the ERDAS configuration of RAMS sets the finest grid spacing at 3 km and classifies the land use at the Complex 41 grid square as water and surrounding grid squares as bog and marsh, evergreen shrub, and short grass. RAMS sets the percent land fraction at Complex 41 to less than 40%. As mentioned earlier, this inaccurate classification significantly affects the RAMS wind field predictions and thus the HYPACT results.

We produced a series of maps and vertical cross-sections at 30 minute intervals to track the HYPACT-predicted plume from just after its release at 1426 UTC to 1700 UTC. The map and cross section at approximately 1.5 hours after the release are shown in Figure 17. Arrows on the map indicate the plume track from Complex 41.

For the first hour after the 1426 UTC release, HYPACT, guided by the light northerly surface winds, moved the plume 3 km south of Complex 41 to a location just southwest of Complex 40 . Vertically, HYPACT kept the plume near the surface and in the layer below 100 meters since RAMS had predicted very little upward motion in this area.

From 1530 to 1630 UTC, HYPACT moved the plume southwest to an area in the western Banana River (Figure 17). HYPACT predicted the plume would begin to rise but stay below 400 meters through 1630 UTC. From 1630 to 1700, HYPACT moved the plume west to the eastern part of Merritt Island where it encountered stronger convection and rose vertically reaching a height of 500 meters.

Comparing the modeled plume trajectory to the actual plume trajectory (based on observations of witnesses), HYPACT performed poorly when Complex 41 was input as the release point. It predicted that the plume would remain close to the ground and move south and west from Complex 41. Witnesses observed the actual plume drift slightly west, rise and then move northward offshore during the one to two hour period after the release. Due to the coarse grid resolution and the resulting inaccurate land use classification in this area, RAMS did not predict significant upward motion thus causing poor HYPACT results.

10 km South of Complex 41 Release Point

For the second HYPACT simulation, we moved the release point 10 kilometers south of Complex 41 to the Cape Canaveral Industrial Area. We picked this point to see how HYPACT would model a release from a grid square where RAMS had not classified the land use as water. The land use classification for the 3 km ∞ 3 km grid square containing the Industrial Area is crop/mixed farming with a percent land fraction of 100%. RAMS predicted strong upward motion in this area.

THIS PAGE INTENTIONALLY LEFT BLANK for figure 17

For the first 30 minutes after the release, HYPACT moved the plume slightly to the northwest to less than 1 km from its source. It remained close to the ground and was lifted to a height of 200 meters. At 1530 UTC, HYPACT began lifting the plume vertically, extending it to a height of over 600 meters by 1600 UTC (Figure 18). Because of the predicted weak sea breeze in the area, HYPACT moved the plume to the north and northwest. HYPACT split the plume as it moved the upper part of the plume faster and more to the north than the lower part of the plume. From 1630 to 1700 HYPACT continued to lift the plume lofting it up to over 700 meters. The upper and lower parts of the plume moved in different directions; the lower part of the plume drifted north-northwest and the upper part moved to the north as the stronger southerly winds aloft began affecting the plume.

Comparing the modeled plume trajectory to the actual plume trajectory (based on observations of witnesses), HYPACT produced a more accurate trajectory when the release location was moved to 10 km south of Complex 41 than it did with the release location at Complex 41. The HYPACT trajectory from the Cape Canaveral Industrial Area was correct in its northward movement and upward lofting. If the modeled plume were transposed to the actual release point at Complex 41 its trajectory would look accurate.

Summary

When HYPACT was run with the release point at Complex 41, it modeled the plume by moving it southwest and never lifted it higher than 400 meters above the surface for the first 2 hours after release. However, when the release point was moved south 10 km, HYPACT handled the plume very differently. HYPACT predicted the plume to move initially to the northwest, but then because of the strong upward vertical motion over the CCAS land area, it lifted the plume to over 700 m above the surface during the 2 hours after the release. Once the plume became elevated, the model's light southerly winds aloft carried the plume to the north. If the path of the plume in this second scenario could be transposed to the actual location of the release at Complex 41, it would closely resemble the actual path of the plume as observed by witnesses at the time of the release.

The difference between the two vastly different HYPACT runs was due to the difference between the way the model characterizes the land use at the release points. Because of the 3 km grid resolution, the model classifies the narrow strip of land where Complex 41 is located primarily as water with a percent land fraction of less than 40%. The model classifies the CCAS land area to the south as crop land with a percent land fraction of 100%. This different land use classification significantly affects RAMS' predictions of surface convergence and vertical motion and turbulence. Based on the results of our analysis, we believe that the model showed promise in modeling the N_2O_4 release and would have produced good results if a smaller grid spacing were used. The smaller grid spacing would better enable RAMS to resolve the complex land use characteristics surrounding Complex 41.

References

Lyons, W.A. and C.J. Tremback, 1994: Final Scientific and Technical Report: Predicting 3-D Wind Flows at Cape Canaveral Air Force Station Using a Mesoscale Model., Contract No. F04701-91-C-0058. Prepared by ASTER/MRC for US Air Force Space and Missile Systems Center, SMC/CLNE, 30 June 1994.

THIS PAGE INTENTIONALLY LEFT BLANK for figure 18

2.6. AMU Chief's Technical Activities (Dr. Merceret)

SLF Wind Measurements Separation Study

After external review, Dr. Merceret's manuscript on the Effects of Spatial Separation on the Validity of Wind Measurements at the Shuttle Landing Facility went to press in mid-January as a NASA Technical Paper. A summary was presented at the 6th Conference on Aviation Weather Systems, Dallas, TX on 18 January 1995.

The results indicate that the proper tool for analyzing wind field differences is structure functions, not correlation functions. Dr. Merceret devised a method of correcting structure functions for differing means and normalizing them even with signals of differing variances.

The data from the SLF indicate that significant real RMS differences exist between wind sensors spaced just a hundred meters apart, and that long term (> 4 h) means may differ by 1 ms^{-1} or more for spacings of less than 500 m. For one-second rate data, spacings on the order of 20 m or less are required to guarantee RMS differences of less than 0.5 ms^{-1}.

SLF Wind Measurements Sheltering Study

Dr. Merceret completed additional measurements at the North site in January. Preliminary results suggest that winds approaching the tree line or parallel to it are affected out less than 100 meters, while winds blowing across the sensor from the direction of the trees are significantly reduced even beyond 400 meters. Additional measurements will be made to define the upper limit of this effect.

Wind Profilers

Dr. Merceret presented the status of the KSC 50 MHz wind profiler to the Workshop on Wind Profiler Planning for US Ranges (Boulder, CO 19-20 October) and participated in the general discussions at the meeting.

Low Temperature LCC Recovery Algorithm

Dr. Merceret wrote a PC-based "proof of concept" program to provide estimates of recovery time based on forecast temperature, wind speed, and relative humidity data. An evaluation copy was supplied to Mr. Ed Priselac at RWO and Mr. John Madura at the KSC Weather Programs Office. The program is initialized with the internal heating, cooling, and solar energy sums from LOWTEMP, the certified PC-based low temperature launch commit criteria recovery software developed last year.

Mesoscale Model Sensitivity

Dr. Merceret and Dr. Taylor met in Boulder on 20 October with representatives from the Environmental Research Laboratory (ERL)/Forecast Systems Laboratory (FSL), Air Force and contractor personnel regarding the ERL/FSL study of the sensitivity of

Mesoscale Numerical Models to instrument placement. Selection of case studies and design of the evaluation protocol were discussed.

3. Project Summary

The MIDDS F-key menu systems developed by Mr. Wheeler have undergone testing, and Mr. Wheeler is currently implementing changes and improvements suggested by the Launch Weather Officers. Mr. Wheeler has also configured the MIDDS terminals in the RWO to display GOES-8 imagery and written utilities to reconfigure the terminals to display GOES-7 imagery should that become necessary.

In order to ensure the integrity of the MIDDS McBasi menu systems, Mr. Wheeler and Ms. Schumann drafted a proposed configuration management plan for the menu systems installed on the RWO terminals. Major Thorp, Commander, RWO Flight, approved the plan in December and requested it be implemented. Mr. Wheeler has since adhered to the steps in the plan for menu system changes as well as for pre-operation menu testing.

After several strong, convective wind gust events occurred near the Shuttle Landing Facility (SLF) on 16 August 1994, the 45th Weather Squadron requested that the AMU determine whether or not the events were microbursts. Mr. Wheeler compared the weather data sets available during the weather events to signatures found by experts during the MIcroburst and Severe Thunderstorm (MIST) project in northern Alabama. During his analysis, Mr. Wheeler found several possible signatures that may help differentiate between Florida's normal summertime thunderstorm days and days associated with potential microburst activity. Mr. Wheeler is collaborating with Mr. Scott Spratt of the NWSO, Melbourne, Florida to write a NWS Technical Attachment that will be submitted to the NWS Southern Region for publication.

The Eastern Range contractor, CSR, has installed and tested the new MIDDS 50 MHz Doppler radar wind profiler decoder for the MSFC wind algorithm data as part of one of their regular McIDAS upgrades. Ms. Schumann assisted in the informal testing of the decoder prior to the formal testing. Captain Scot Heckman of the 45th Weather Squadron provided operational DRWP support for the launch attempt and subsequent launch on 20 and 22 December.

The Air Force is currently procuring a network of boundary layer profilers for the CCAS/KSC area. The network is being designed and developed by NYMA, Inc. and is based on the LAP□ - 3000 Doppler radar wind profiler developed by Radian Corporation and Sonoma Technology under a Cooperative Research and Development Agreement (CRDA) with NOAA. The LAP□ - 3000 radar has an operating frequency of 915 MHz, a peak power of 500 watts, and a five beam electrically steered phased-array antenna with clutter fence. The profilers will provide wind estimates from approximately 120 m to 2 to 4 km above the surface with range gate spacing of 60 to 400 m and averaging periods of 3 to 60 minutes. Radian claims the wind speed accuracy to be ~1 ms^{-1} and the wind direction accuracy to be ~10□.

In addition to wind profiles, each radar will contain a Radio Acoustic Sounding System (RASS) which uses four acoustic horns to provide profiles of virtual temperature from approximately 120 m to 1.5 km above the surface. Radian claims the virtual temperature accuracy to be ~1□ C.

Although the system is being designed to support up to 15 profilers, the initial configuration of the network will contain five profilers installed in a diamond-shaped pattern centered on KSC. The first profiler was installed at the False Cape site in October 1994 and the second profiler was installed at the South Cape site in January 1995. Profilers are to be installed at the remaining three sites by the summer of 1995. NYMA is currently designing and developing a system to ingest, process, and display data from all five profilers.

Dr. Taylor performed a preliminary comparison of the 10 minute consensus averaged wind profiles from the False Cape profiler and 11 time-proximate rawinsonde profiles from CCAS weather station during the period 01-04 December 1994. The results of the analysis are discussed in the body of this report. Though the data set analyzed is too small for producing conclusions about profiler performance, the analysis suggests that the profiler is performing as expected, but there is a need for post-processing quality control of the wind estimates and/or more advanced signal processing techniques.

The archiving of real-time MASS model runs for the purpose of model evaluation is complete. All available coarse and fine grid forecasts and observations from 15 January 1994 through 15 October 1994 are being used for model verification. The AMU continues to run MASS in real-time so that model initialization and forecast products can be transferred back to MIDDS for examination by RWO, SMG, and NWS forecasters. The transfer of MASS output to MIDDS occurs after the forecasts have expired so that initialization and forecast products can not be used for operational decisions. In addition, the model runs are still being archived so that Model Output Statistics (MOS) can be generated from the largest possible sample of real-time cases.

Ms. Yersavich has processed data to yield statistics on the number of completed MASS model runs compared with the number of total possible runs for the entire archiving period from January through October 1994. 10.9% of the coarse runs were lost due to hardware problems, 2.4% due to software problems, and 2.4% due to loss of data. No model forecasts were lost due to instabilities generated by the model's physics or dynamics since December 1993 when the AMU started running MASS in a real-time configuration. These results suggest that MASS is extremely robust and would be a very reliable operational system.

Dr. Manobianco completed the analysis of MASS model forecast errors at three rawinsondes sites in Florida for 45 km and 11 km MASS runs, NGM B-grid (~190 km) runs, and persistence forecasts for the entire archive period (January - October 1994). He also examined MASS model forecasts of stability indices and precipitable water for the same period. Dr. Manobianco presented these results at the Sixth Conference on Aviation Weather Systems held in Dallas, TX from 15-20 January 1995.

The average bias and RMSE were computed from twice daily rawinsonde data for three sites over Florida from 15 January 1994 to 15 October 1994. The MASS model coarse and fine grid analysis (0 h) bias and RMSE for temperature and wind speed are typically smaller than those from the NGM indicating that the MASS analysis scheme fits the rawinsonde data more closely. By 12 h, the errors in the NGM and MASS forecasts for temperature, moisture, and wind at 850 mb, 500 mb, and 300 mb are similar in magnitude. The MASS model predictions of stability based on K Index are more accurate

when the soundings are more unstable (i.e. higher K Index values). In general, MASS is predicting the large scale features that are sampled by twice-daily rawinsonde observations as well as the NGM. This result is not surprising since the NGM provides boundary conditions for the coarse grid and the coarse grid provides boundary conditions for fine grid. Under strong inflow conditions, the information introduced at the boundary of the coarse or fine grid domains can impact the forecasts in a relatively short time period.

The higher resolution MASS model should show more skill than current operational models like the NGM in predicting mesoscale features such as the sea breeze. Mesoscale model validation requires mesoscale data. Therefore, the AMU is in the process of verifying the coarse and fine grid forecasts of the sea breeze, convective precipitation, and tropospheric winds above 2 km using hourly measurements from the KSC/CCAS wind towers (~5 km average spacing), Florida Water Management and KSC/CCAS rain gauges (~10 km average spacing), and KSC 50 MHz Doppler wind profiler, respectively.

The primary AMU activity during the past quarter on the Emergency Response Dose Assessment System (ERDAS) model evaluation was the preparation of a memorandum describing the AMU's modeling of a nitrogen tetroxide release from Complex 41 on 20 August 1994. The AMU used the accident as a case study for evaluating ERDAS' ability to model the release and accurately predict the location and concentration of the plume. We evaluated output from both of the major models within ERDAS–the meteorological model, RAMS (Regional Atmospheric Modeling System), and the diffusion model, HYPACT (Hybrid Particle and Concentration Transport).

The 3-km resolution of the land use in the ERDAS RAMS configuration significantly affected the modeling of the N_2O_4 release at Complex 41. The narrow strip of land where Complex 41 is located is approximately 1½ to 4 km wide, bounded on the west by the Banana River and on the east by the Atlantic Ocean. The land use in the area is very complex due to the oceans, estuaries, swamps and vegetated land. RAMS attempts to apply a single land use class and percent land area to each 3 km x 3 km grid square. RAMS classified the grid square where Complex 41 is located as inland water or ocean (Classes 14 and 15) with a percent land fraction of less than 40%. The grid squares surrounding the Complex 41 grid square were classified as bog and marsh (Class 13), evergreen shrub (Class 16), and short grass (Class 2). This inaccurate classification can lead to inaccurate modeling of horizontal and vertical velocities and turbulence.

When HYPACT was run with the release point at Complex 41, it modeled the plume by moving it southwest and never lifted it higher than 400 meters above the surface for the first 2 hours after release. However, when the release point was moved south 10 km, HYPACT handled the plume very differently. HYPACT predicted the plume to move initially to the northwest, but then because of the strong upward vertical motion over the CCAS land area, it lifted the plume to over 700 m above the surface during the 2 hours after the release. Once the plume became elevated, the model's light southerly winds aloft carried the plume to the north. If the path of the plume in this second scenario could be transposed to the actual location of the release at Complex 41, it would closely resemble the actual path of the plume as observed by witnesses at the time of the release.

Dr. Merceret circulated the revised draft of the separation study technical memorandum for external review and has since updated the draft accordingly. The technical memorandum was submitted for publication as an official NASA Technical Paper in mid January. Dr. Merceret presented the results of the SLF wind measurements study at the 6th Conference on Aviation Weather Systems in Dallas, TX on 18 January 1994.

Attachment 1: AMU FY-94 Tasks

Task 1 AMU Operations

- Operate the AMU. Coordinate operations with NASA/KSC and its other contractors, 45th Space Wing and their support contractors, the NWS and their support contractors, other NASA centers, and visiting scientists.

- Establish and maintain a resource and financial reporting system for total contract work activity. The system shall have the capability to identify near-term and long-term requirements including manpower, material, and equipment, as well as cost projections necessary to prioritize work assignments and provide support requested by the government.

- Monitor all Government furnished AMU equipment, facilities, and vehicles regarding proper care and maintenance by the appropriate Government entity or contractor. Ensure proper care and operation by AMU personnel.

- Identify and recommend hardware and software additions, upgrades, or replacements for the AMU beyond those identified by NASA.

- Prepare and submit in timely fashion all plans and reports required by the Data Requirements List/Data Requirements Description.

- Prepare or support preparation of analysis reports, operations plans, presentations and other related activities as defined by the COTR.

- Participate in technical meetings at various Government and contractor locations, and provide or support presentations and related graphics as required by the COTR.

- Design McBasi routines to enhance the usability of the MIDDS for forecaster applications at the RWO and SMG. Consult frequently with the forecasters at both installations to determine specific requirements. Upon completion of testing and installation of each routine, obtain feedback from the forecasters and incorporate appropriate changes.

Task 2 Training

- Provide initial 40 hours of AMU familiarization training to Senior Scientist, Scientist, Senior Meteorologist, Meteorologist, and Technical Support Specialist in accordance with the AMU Training Plan. Additional familiarization as required.

- Provide KSC/CCAS access/facilities training to contractor personnel as required.

- Provide NEXRAD training for contractor personnel.

• Provide additional training as required. Such training may be related to the acquisition of new or upgraded equipment, software, or analytical techniques, or new or modified facilities or mission requirements.

Task 3 Improvement of 90 Minute Landing Forecast

• Develop databases, analyses, and techniques leading to improvement of the 90 minute forecasts for STS landing facilities in the continental United States and elsewhere as directed by the COTR.

• Subtask 2 - Fog and Stratus At KSC

•• Develop a database for study of weather situations relating to marginal violations of this landing constraint. Develop forecast techniques or rules of thumb to determine when the situation is or is not likely to result in unacceptable conditions at verification time. Validate the techniques and transition to operations.

Subtask 4 - Forecaster Guidance Tools

•• The 0.2 cloud cover sub task is extended to include development of forecaster guidance tools including those based on artificial neural net (ANN) technology.

Task 4 Instrumentation and Measurement Systems Evaluation

• Evaluate instrumentation and measurement systems to determine their utility for operational weather support to space flight operations. Recommend or develop modifications if required, and transition suitable systems to operational use.

• Subtask 3 - Doppler Radar Wind Profiler (DRWP)

•• Evaluate the current status of the DRWP and implement the new wind algorithm developed by MSFC. Operationally test the new algorithm and software. If appropriate, make recommendations for transition to operational use. Provide training to both operations and maintenance personnel. Prepare a final meteorological validation report quantitatively describing overall system meteorological performance.

• Subtask 4 - Lightning Detection and Ranging (LDAR) System

•• Evaluate the NASA/KSC Lightning Detection and Ranging (LDAR) system data relative to other relevant data systems at KSC/CCAS (e.g., LLP, LPLWS, and NEXRAD). Determine how the LDAR information can be most effectively used in support of NASA/USAF operations. If appropriate, transition to operational use.

• Subtask 5 - Melbourne NEXRAD

•• Evaluate the effectiveness and utility of the Melbourne NEXRAD (WSR-88D) operational products in support of spaceflight operations. This work will be coordinated with appropriate NWS/FAA/USAF personnel.

- Subtask 7 - ASOS Evaluation

•• Evaluate the effectiveness and utility of the ASOS data in terms of spaceflight operations mission and user requirements.

- Subtask 9 - Boundary Layer Profilers

•• Evaluate the meteorological validity of current site selection for initial 5 DRWPs and recommend sites for any additional DRWPs (up to 10 more sites). Determine, in a quantitative sense, advantages of additional DRWPs. The analysis should determine improvements to boundary layer resolution and any impacts to mesoscale modeling efforts given additional DRWPs. Develop and/or recommend DRWP displays for operational use.

- Subtask 10 - NEXRAD/McGill Inter-evaluation

•• Determine whether the current standard WSR-88D scan strategies permit the use of the WSR-88D to perform the essential functions now performed by the PAFB WSR-74C/McGill radar for evaluating Flight Rules and Launch Commit Criteria (including the proposed VSROC LCC).

Task 5 Mesoscale Modeling

- Evaluate Numerical Mesoscale Modeling systems to determine their utility for operational weather support to space flight operations. Recommend or develop modifications if required, and transition suitable systems to operational use.

- Subtask 1 - Evaluate the NOAA/ERL Local Analysis and Prediction System (LAPS)

•• Evaluate LAPS for use in the KSC/CCAS area. If the evaluation indicates LAPS can be useful for weather support to space flight operations, then transition it to operational use.

- Subtask 2 - Install and Evaluate the MESO, Inc. Mesoscale Forecast Model

•• Install and evaluate the MESO, Inc. mesoscale forecast model for KSC being delivered pursuant to a NASA Phase II SBIR. If appropriate, transition to operations.

- Subtask 3 - Acquire the Colorado State University RAMS Model

•• Acquire the Colorado State University RAMS model or its equivalent tailored to the KSC environment. Develop and test the following model capabilities listed in priority order:

1) Provide a real-time functional forecasting product relevant to Space shuttle weather support operations with grid spacing of 3 km or smaller within the KSC/CCAS environment.

2) Incorporate three dimensional explicit cloud physics to handle local convective events.

3) Provide improved treatment of radiation processes.

4) Provide improved treatment of soil property effects.

5) Demonstrate the ability to use networked multiple processors.

Evaluate the resulting model in terms of a pre-agreed standard statistical measure of success. Present results to the user forecaster community, obtain feedback, and incorporate into the model as appropriate. Prepare implementation plans for proposed transition to operational use if appropriate.

- Subtask 4 - Evaluate the Emergency Response Dose Assessment System (ERDAS)

•• Perform a meteorological and performance evaluation of the ERDAS. Meteorological factors which will be included are wind speed, wind direction, wind turbulence, and the movement of sea-breeze fronts. The performance evaluation will include:

1) Evaluation of ERDAS graphics in terms of how well they facilitate user input and user understanding of the output.

2) Determination of the requirements that operation of ERDAS places upon the user.

3) Documentation of system response times based on actual system operation.

4) Evaluation (in conjunction with range safety personnel) of the ability of ERDAS to meet range requirements for the display of toxic hazard corridor information.

5) Evaluation of how successfully ERDAS can be integrated in an operational environment at CCAS.